

## Interannual Variability of Water Circulation Regimes in the Arctic Ocean

E. E. Lemeshko

*Marine Hydrophysical Institute of RAS, Sevastopol, Russia  
e-mail: e.lemeshko@mhi-ras.ru*

### Abstract

The article studies the interannual variability of the Arctic Ocean water circulation regimes according to altimetry data for the area from 65°N to 89.75°N including the ice-covered area of the ocean. The purpose of the work is to study the variability of the ocean level and the velocities of surface geostrophic currents depending on the value of the Arctic oscillation index, and to establish quantitative patterns between them. In addition, the paper considers the influence of different ocean circulation regimes and the value of the Arctic oscillation index on the steric level variability as an indicator of freshening/salinization processes in the polar region north of 81.5°N. The steric component of level was calculated as the difference between the dynamic topography from altimetry data and the GRACE data of the manometric level component. On an interannual time scale, the sea level response averaged over the Arctic Ocean is in antiphase with the Arctic Oscillation Index. Based on the method of multiple regression, quantitative estimates of the dependence of the sea level and geostrophic velocity components on the value of the Arctic oscillation index were obtained. The level difference between the shelf and the deeper part of the ocean was ~ 4 cm per unit of the Arctic oscillation index. The difference between the areas of positive and negative values of the sea level anomalies creates a pressure gradient, which leads to an increase in the anomalies of surface geostrophic velocities and enhances the inflow of Atlantic waters along the shelf edge in an easterly direction during the cyclonic regime (Arctic Oscillation Index is greater than 0). Under the anticyclonic regime of atmospheric circulation (the index is less than 0), the effect becomes opposite. This agrees with the estimates of the linear regression coefficients for the velocity anomalies of geostrophic currents, which amounted to ~ 0.5 cm/s per 1 index unit. On the basis of the obtained results, a conceptual scheme of the regimes of circulation and distribution of desalinated waters depending on the phase of the Arctic oscillation is proposed.

**Keywords:** Arctic Ocean, altimetry, steric level, arctic oscillation, ocean circulation regimes, altimetry, GRACE

**Acknowledgements:** The work was funded by the RFBR under research project no. 20-35-90061.

**For citation:** Lemeshko, E.E., 2023. Interannual Variability of Water Circulation Regimes in the Arctic Ocean. *Ecological Safety of Coastal and Shelf Zones of Sea*, (1), pp. 48–64. doi:10.29039/2413-5577-2023-1-48-64

© Lemeshko E. E., 2023



This work is licensed under a Creative Commons Attribution-Non Commercial 4.0 International (CC BY-NC 4.0) License

---

# Межгодовая изменчивость режимов циркуляции вод Северного Ледовитого океана

Е. Е. Лемешко

Морской гидрофизический институт РАН, Севастополь, Россия  
e-mail: e.lemeshko@mhi-ras.ru

## Аннотация

Статья посвящена изучению межгодовой изменчивости режимов циркуляции вод Северного Ледовитого океана по данным альтиметрии для области от  $65^{\circ}$  до  $89.75^{\circ}$  с. ш., включая область океана, покрытую льдом. Цель работы заключается в исследовании изменчивости уровня океана и скоростей поверхностных геострофических течений в зависимости от величины индекса арктической осцилляции, а также в установлении количественных закономерностей между ними. Дополнительно рассмотрено влияние различных режимов циркуляции океана и величины индекса арктической осцилляции на изменчивость стерического уровня как индикатора процессов распреснения/осолонения в полярной области севернее  $81.5^{\circ}$  с. ш. Стерическая компонента уровня рассчитывалась как разница между динамической топографией по данным альтиметрии и данными *GRACE* о манометрической компоненте уровня. На межгодовом масштабе временной изменчивости отклик уровня моря, осредненного по Северному Ледовитому океану, находится в противофазе с индексом арктической осцилляции. На основе метода множественной регрессии получены количественные оценки зависимости уровня моря и компонент геострофической скорости от величины индекса арктической осцилляции. Перепад уровня между шельфом и более глубоководной частью океана составил  $\sim 4$  см на 1 единицу индекса арктической осцилляции. Разница между областями положительных и отрицательных значений аномалий уровня моря создает градиент давления, что приводит к увеличению аномалий поверхностных геострофических скоростей и усиливает поступление атлантических вод вдоль кромки шельфа в восточном направлении при циклоническом режиме (индекс арктической осцилляции больше нуля). При антициклоническом режиме циркуляции атмосферы (индекс меньше нуля) эффект становится противоположным. С этим согласуются оценки коэффициентов линейной регрессии для аномалий скорости геострофических течений, которые составили  $\sim 0.5$  см/с на 1 единицу индекса. На основании полученных результатов предложена концептуальная схема режимов циркуляции и распространения распресненных вод в зависимости от фазы арктической осцилляции.

**Ключевые слова:** Северный Ледовитый океан, альтиметрия, стерический уровень, арктическая осцилляция, режимы циркуляции океана, *GRACE*

**Благодарности:** работа выполнена при финансовой поддержке РФФИ в рамках научного проекта № 20-35-90061.

**Для цитирования:** Лемешко Е. Е. Межгодовая изменчивость режимов циркуляции вод Северного Ледовитого океана // Экологическая безопасность прибрежной и шельфовой зон моря. 2023. № 1. С. 48–64. EDN TYGZLF. doi:10.29039/2413-5577-2023-1-48-64

## Introduction

The Arctic Ocean near-surface circulation is mainly characterized by the alternation of anticyclonic and cyclonic phases on interannual variability scales [1–3]. Such a description of the circulation was based on the analysis of the dynamic topography calculated from the data of hydrological observations, as well as on numerical modelling [1–3]. According to modern field studies, the most dramatic changes in the Arctic Ocean occurred in the 2010s [1].

The area around the North Pole (NP) north of 81.5°N, sometimes called a “blind” spot (NP area in Fig. 1) due to the lack of any altimetry data there until 2011, is important for understanding hydrophysical changes in the Arctic Ocean. Sea ice and desalinated surface waters are carried by the Transpolar Drift (TPD) through this region towards the North Atlantic and largely determine the thermohaline structure of its subpolar regions. Therefore, such parameters as ice thickness, bottom pressure, and steric level (reflecting the vertical hydrological structure of waters) are key indicators of the variability of the entire Arctic Ocean.

Independent assessments of the freshwater balance based on the analysis of hydrological data showed two independent trends in the variability of the Arctic Ocean freshwater balance [4]. On the one hand, freshening was observed in the Canadian basin with a rate of change in the freshwater layer thickness of  $2.04 \pm 0.64$  m/10 years, and on the other hand, salinization was observed in the East Eurasian basin with a trend of  $0.96 \pm 0.86$  m/10 years [4]. According to long-term hydrological observations, freshening was also noted in the North Pole region with a trend of  $1.19 \pm 0.02$  m/10 years [4].

As a result of the analysis of complex data from field studies in the area of the Beaufort Gyre, it was concluded that the fresh water supply increased by 40 % from 2003 to 2018 compared to the long-term average for 1970–2000. Accumulation of fresh water due to the impact of anticyclonic atmospheric circulation was considered as the main mechanism of freshening [5].

Based on the results of sea level analysis according to altimetry data for the area of the Beaufort Gyre and the North Sea, opposite level trends of 2009–2011 were identified. [6]. As a result, it was concluded that the shift in sea level variability in these areas took place due to changes in large-scale atmospheric circulation associated with the Arctic Oscillation (AO) Index [5, 6].

The Arctic Oscillation (AO) is a climate index that characterizes the distribution of atmospheric pressure and peculiarities of the wind field over the Arctic. When most of the Arctic is occupied by a cyclone, the AO Index is positive. It becomes negative during the anticyclonic circulation of the atmosphere. During the positive phase of the AO Index, the inflow of warm Atlantic waters increases and the distribution of the Pacific waters weakens. In addition, the transport of sea ice and near-surface desalinated waters to the Atlantic increases, and the distribution routes of the runoff of the Eurasian rivers change. During the negative phase of the AO Index, an anticyclonic pressure area is located over the Arctic,

and the sign of the current discharge anomaly changes to the opposite one [2]. The ocean circulation cyclonic mode lags behind the AO Index by about 1 year [7–9].

The article studies the variability of the ocean level and the velocities of surface geostrophic currents depending on the value of the AO Index, as well as the establishment of quantitative patterns between them. In addition, the paper considers the influence of different ocean circulation regimes and the value of the AO Index on the steric level variability as an indicator of freshening/salinization processes in the area of the Beaufort Gyre and in the polar region north of 81.5°N. The reconstructed steric component of level was calculated as the difference between the dynamic topography from altimetry data and the GRACE data of the manometric level component. Then, the reconstructed steric level was averaged over the area of the Beaufort Gyre and over the blind polar area north of 81.5°N, which was inaccessible to satellite altimetry until 2011 (Fig. 1).

### Data and Methods

After 2011, new Envisat and CryoSat-2 satellites were launched in high-altitude orbits, which receive altimetry data in the “blind” spot area up to 89.75°N and improve the accuracy of anomalous sea level measurements [9].

Methodological work was carried out to compare altimetry data with sea level measurements using coastal tide gauges. The results showed a fairly high degree of correlation between them for periods of open water: in the Norwegian Sea, the average values were 0.86 [9, 10], and in the Barents Sea, 0.89 [2].

The obtained new altimetry data were used to estimate the dynamic topography of the entire Arctic Ocean, including the area north of 81.5°N, according to the following formula:

$$H_{DT} = H_{SSH} - H_G, \quad (1)$$

where  $H_{DT}$  – dynamic ocean topography;  $H_{SSH}$  – sea surface height;  $H_G$  – geoid surface height [9, 10]. Surface geostrophic velocities were calculated from the  $H_{DT}$  dynamic topography values obtained by formula (1) [10, 11].

Two arrays of satellite altimetry data in the form of monthly average data of dynamic ocean topography and surface geostrophic velocities provided by the Centre for Polar Observation and Modelling, University College London ([www.cpom.ucl.ac.uk/dynamic\\_topography](http://www.cpom.ucl.ac.uk/dynamic_topography)), were used in the paper. The first array consists of the data for 2003–2014 covering from 65° to 81.5°N on a grid of 0.75° × 0.25° [11], and the second array includes the data for 2011–2020 with a higher resolution (20 × 20 km) on a polar stereographic grid covering from 65° to 89.75°N. Both arrays include data concerning ocean areas covered with ice. The description of the method for calculating sea level is given in [10].

In addition, gravimetry data (Gravity Recovery And Climate Experiment (GRACE)), version RL06, grid 1° × 1°, monthly averages, 2002–2017, and GRACE-FO, 2018–2021, covering the entire ocean up to 89.9°N, were used (<https://podaac.jpl.nasa.gov/datasetlist?search=tellus>).

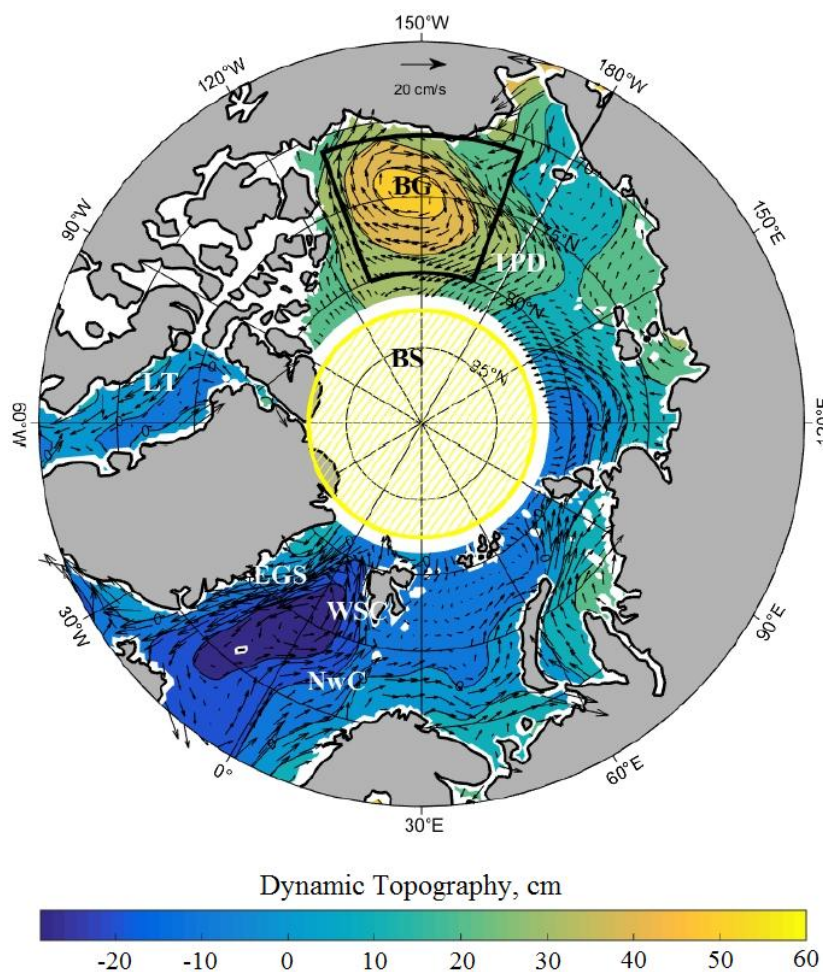


Fig. 1. Scheme of the surface currents of the Arctic Ocean: dynamic topography and geostrophic currents averaged from altimetry data for 2003–2014. BS – “blind” spot – the region north of 81.5°N; NwC – Norwegian Current; LT – Labrador Current; WSC – West Spitsbergen Current; EGC – East Greenland Current; TPD – Transpolar Drift; BG – Beaufort Gyre

### Results

For the Arctic Ocean, the mean values of dynamic topography and surface geostrophic velocities for 2003–2014 were calculated (Fig. 1). Figure 1 illustrates the following main currents and large-scale elements of the ocean circulation marked with white symbols: the Norwegian Current, the Labrador Current, the West Spitsbergen Current, the East Greenland Current, the Transpolar Drift, and the Beaufort

Gyre (Fig. 1), which correspond to the known pattern of currents <sup>1)</sup> and to the estimates of geostrophic velocities obtained for these regions from earlier altimetry products [10].

The average current velocities calculated by us for the period 2003–2014 are ~ 10 and ~ 15 cm/s in the area west of Spitsbergen and near Novaya Zemlya, respectively. The level difference between the shelf and the deep part of the basin reaches 30 cm (Fig. 1).

In addition, when compared with the data of current meters at ten mooring buoys for 2011–2018, the correlation value for the Laptev Sea and the Beaufort Sea was 0.7, and for the Fram Strait it was 0.34. At the same time, the root-mean-square (RMS) deviations between the modules of geostrophic current velocities according to altimetry data and contact measurements by ADCP at mooring buoys amounted to 1–2 cm/s, and the RMS deviations of the difference in angle values were about 60° for 2005–2008 [10].

To analyze the interannual sea level variability, intraseasonal fluctuations were removed using a moving average filter with a window width of 12 months, then series of sea level anomalies were formed as deviations from their long-term average values. Figure 2 shows the obtained sea level anomalies averaged over the entire Arctic Ocean.

Both altimetry arrays are in good agreement with each other in the 2011–2014 data overlap interval (Fig. 2).

Anticyclonic regimes in the Arctic Ocean identified by positive sea level anomalies  $H_{DT}$  were observed in 2006–2007, 2009–2013, and 2016–2017 (Fig. 2).

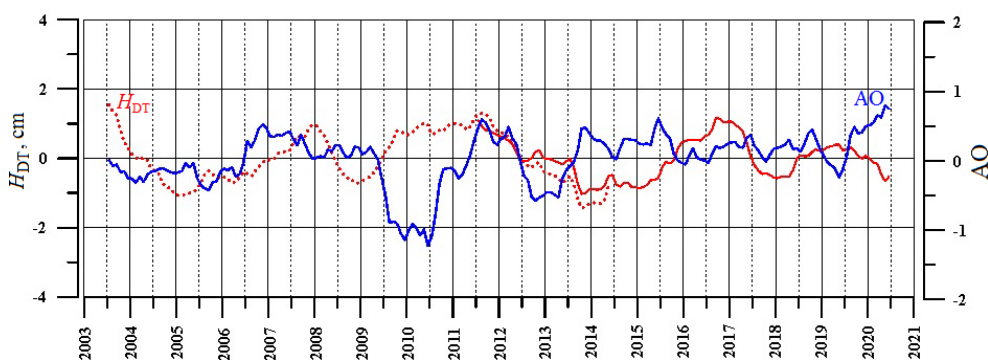


Fig. 2. Plots of dynamic topography averaged over the Arctic Ocean (cm) according to altimetry data ( $H_{DT}$ ) for the period 2003–2014 (red dashed line), for the period 2011–2020 (red solid line) and the Arctic Oscillation (AO) Index (blue line) after filtering by a moving average with a window width of 12 months

<sup>1)</sup> Treshnikov, A.F., 1985. [Arctic Atlas]. Moscow: Glavnoe Upravlenie Geodezii i Kartografii, 204 p. (in Russian).

Cyclonic regimes (negative level anomalies) were observed in 2005, 2008, and 2014 (Fig. 2). For the entire period of altimetry observations for 2003–2020, the maximum duration of the anticyclonic regime of the ocean was ~ 3.5 years in 2009–2013, and this corresponded to the negative phase of the AO Index (Fig. 2). Conversely, during the positive phase of the AO Index (2013–2016), when the cyclonic regime is identified in the surface atmospheric pressure field, negative values of sea level anomalies are observed with a maximum duration of ~2.5 years (Fig. 2).

The AO Index data provided by NOAA/NWS Climate Prediction Center (USA)<sup>2)</sup>, were used in the paper. Long periods of the AO Index negative phase can be observed in 2003–2006, 2009–2011, 2012–2013, and 2016–2017. This corresponds to the anticyclonic circulation in the Arctic Ocean: average values of dynamic topography over the water area are positive (Fig. 2). For the AO Index positive phase, negative values of the dynamic topography averaged over the Arctic Ocean are observed, most pronounced in 2013–2016 (Fig. 2). During the period when the cyclonic regime prevailed in the atmosphere during the AO positive phase, the cyclonic circulation of the ocean manifested itself in a decrease in the mean sea level with a time delay of about 1 year relative to the AO Index phase (Fig. 2).

Sea level  $H$  consists of the sum of steric level component  $H_{\text{Sth}}$  stipulated by seawater density changes, and manometric level component  $H_{\text{man}}$  stipulated by variations in the water mass of the liquid column, with their different characteristic time scales of variability [12, 13]:

$$H = H_{\text{Sth}} + H_{\text{man}} . \quad (2)$$

The variability of the manometric level in the Norwegian and Barents Seas is mainly intraseasonal in nature, and its contribution reaches 80 % of the total dispersion. Therefore, the barotropic response of sea level to wind forcing has a scale of several months and can be masked by longer-term steric level variability.

In papers [12, 13], based on the analysis of GRACE data and numerical modelling, it was found that on the intraseasonal scales, the variations in the manometric sea level had a high correlation with the anomalies of the wind field for the sector under consideration.

To analyze the interannual variability of dynamic topography data and surface geostrophic velocities, a linear trend was removed from the data at each grid point after filtering by the moving average with the window width of 12 months. The resulting ocean level anomalies were averaged over the periods of the positive ( $AO > 0$ ) and negative ( $AO < 0$ ) phases of the AO Index [14]. First, such an approach was tested for the ocean sector ( $65^{\circ}$ – $81.5^{\circ}$ N,  $0^{\circ}$ – $70^{\circ}$ E) that includes

---

<sup>2)</sup> NWS. *Arctic Oscillations*. 202. [online] Available at: [http://www.cpc.ncep.noaa.gov/products/precip/CWlink/daily\\_ao\\_index/ao.shtml](http://www.cpc.ncep.noaa.gov/products/precip/CWlink/daily_ao_index/ao.shtml) [Accessed: 30 March 2023].

the North, Norwegian, and Barents Seas for 2003–2014 [9]. During the periods when the AO Index is in its positive phase, the central part of the Arctic Ocean is occupied by a cyclonic area with negative values of level anomalies up to  $-3$  cm, the zero level isoline corresponds approximately to the isobath of 300 m. In the southern part of the Barents Sea and in the Kara Sea, positive level anomalies up to 3 cm are distinguished; the vectors of velocity anomalies ( $\sim 1$  cm/s) correspond to the cyclonic circulation regime. For the periods when the AO Index was in its negative phase, the anomalies of the ocean level and velocities corresponded to the anticyclonic circulation regime. Similarly, for the entire water area of the Arctic Ocean for 2011–2020, the cyclonic circulation regime of the ocean during the positive phase of the AO Index  $> 0$  and the anticyclonic circulation regime during the negative phase of the AO Index  $< 0$  were distinguished.

To estimate quantitatively the effect of the AO Index on the variability of sea level anomalies  $H_{DT}$  and surface geostrophic velocities  $U$ ,  $V$ , linear regression analysis [15] was used:

$$\begin{aligned} H_{DT}^i &= \alpha_{DT}^i \cdot AO + \varepsilon_{DT}^i, \\ U^i &= \alpha_U^i \cdot AO + \varepsilon_U^i, \\ V^i &= \alpha_V^i \cdot AO + \varepsilon_V^i, \end{aligned} \quad (3)$$

where regression coefficients for level  $\alpha_{DT}^i$ , cm, and velocity component  $\alpha_U^i$ ,  $\alpha_V^i$ , cm/s, were estimated at each  $i$ -th node of the grid, and  $\varepsilon_{DT}^i$ ,  $\varepsilon_U^i$ ,  $\varepsilon_V^i$  are uncorrelated white noise. Figure 3 shows the sea level regression coefficients in the form of isolines and the corresponding coefficients of the current velocity modulus in the form of vectors  $\alpha_{modV}^i$ :

$$\alpha_{modV}^i = [(\alpha_U^i)^2 + (\alpha_V^i)^2]^{1/2}. \quad (4)$$

The spatial distribution of the coefficients of linear regression of the sea level and surface geostrophic velocities corresponds to the cyclonic circulation regime in the Arctic Ocean at positive values of the AO Index according to expression (3) (Fig. 3) and, thus, is consistent with the distribution of the sea level and velocities averaged for the positive phase of the AO Index. Similarly, for the negative phase of the AO Index, the distribution of the linear regression coefficients of the sea level and surface velocities changes sign to minus according to (3), which gives an anticyclonic pattern of circulation and is consistent with the map of sea level values and current velocities averaged over periods of the negative phase of the AO Index. To increase the robustness of the regression estimates, the linear trend was eliminated from the data of the AO Index, dynamic topography, and velocities after filtering by the moving average with the window width of 12 months. The anomalies obtained in this way were processed according to regression formula (3), and the results are shown in Figs. 3, 4.



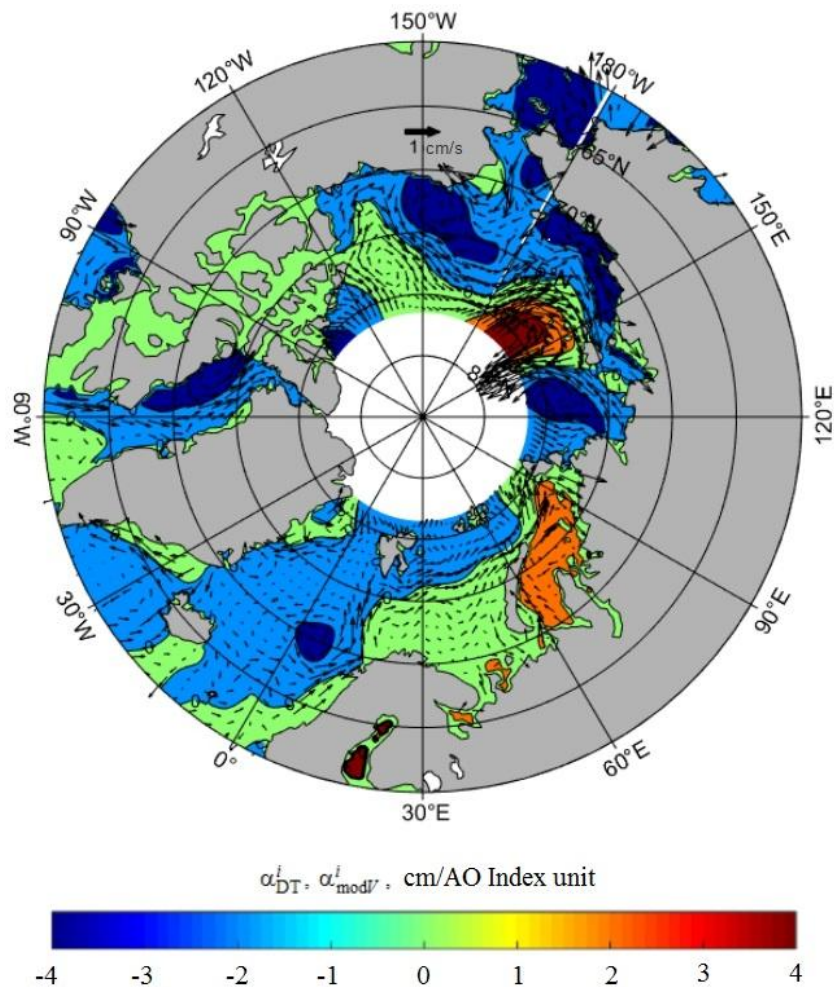


Fig. 3. Spatial distribution of linear regression coefficients for sea level anomalies  $\alpha_{DT}^i$  (cm/AO Index unit) and for current velocity anomalies ((cm/s)/AO Index unit) as vectors for 2003–2014

As a result, regression relations for the sea level and geostrophic velocity components depending on the value of the AO Index were obtained. Calculated linear regression coefficients  $\alpha_{DT}^i$  for sea level anomalies are more than  $\sim 2$  cm in the shelf zone and about  $-2$  cm in the deep part of the ocean (Fig. 3).

For the Norwegian Sea, the northern part of the Barents and Kara Seas, for the shelf of the Laptev Sea and the East Siberian Sea, the coefficients of linear regression of the modulus of current velocity anomalies  $\alpha_{modV}^i$  have values of  $\sim 0.5$  cm/s per AO Index unit concerning altimetry data for 2003–2014 and  $0.6 \div 0.8$  cm/s per AO Index unit concerning data for 2011–2020 (Fig. 3).

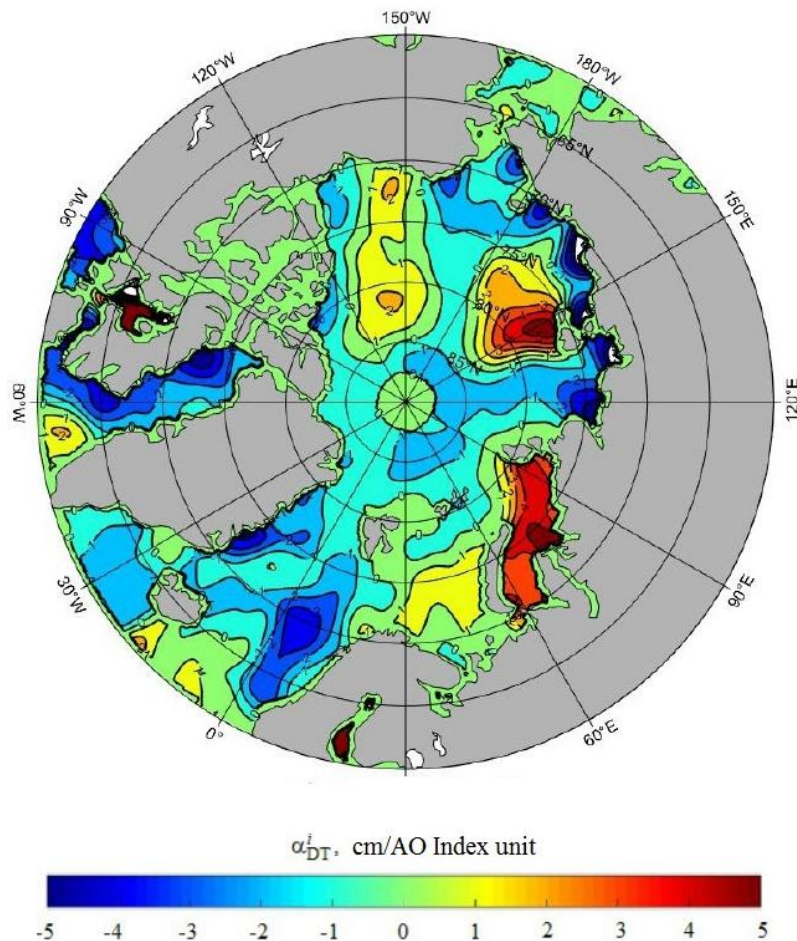


Fig. 4. Spatial distribution of linear regression coefficients for sea level anomalies (cm/AO Index unit) for 2011–2020

For the “blind” spot 81.5°–89°N in the sector 30°–80°E and 130°–180°E, high values of the coefficients were also noted (0.6–0.8 cm/s per AO Index unit), and in the sector 120° W – 30°E, on the contrary, low values (0.1–0.2 cm/s per AO Index unit) were observed (Fig. 4).

The sea level difference between the shelf and the deeper part is ~ 4 cm/AO Index unit (Fig. 4). This difference intensifies in the Kara Sea to ~ 5 cm, and in the Laptev and East Siberian Seas to ~ 8 cm/AO Index unit in the 150°–180°E sector (Fig. 4).

An increase in sea level gradients leads to an increase in pressure gradients between the shelf and the deeper part of the ocean and, as a result, to an increase

in geostrophic velocities up to  $\sim 1.5$  cm/s per AO Index unit (Fig. 4). Consequently, during the positive AO phase, there is an increase in the transport of fresh water from the shelf of the Laptev Sea and the East Siberian Sea to the central part of the ocean.

Thus, during the positive phase of the AO Index, when the central part of the Arctic is occupied by a cyclone, there is an increase in the magnitude of current velocity anomalies, which contributes to the inflow of warm Atlantic waters into the Barents Sea and the central part of the ocean, and a decrease in the inflow of waters through the Bering Strait is also observed. During the negative AO phase, when an anticyclonic pressure area is located over the Arctic, the signs of the current velocity anomaly reverse, which reduces the inflow of warm Atlantic waters into the Arctic Ocean and increases the inflow of Pacific waters through the Bering Strait.

Altimetry and GRACE data were used to estimate the manometric component of the Arctic Ocean level. Manometric level  $H_{\text{man}}$  is stipulated by the variations of the water column mass. Ocean level  $H$  is determined by altimetry data. Thus, the reconstructed steric component of sea level  $H_{\text{sh}}$  is equal to sea level  $H$  minus the manometric component of the level. Using relation (2), the steric level fields were reconstructed in accordance with altimetry and GRACE data. The reconstructed steric level was compared with the steric level calculated from the hydrological data (Unified Database for Arctic and Subarctic Hydrography, UDASH, Available at <https://doi.pangaea.de/10.1594/PANGAEA.872931>). It was shown in [4, 5] that the contribution of the halosteric component prevails over the thermosteric component in the steric level of the Arctic Ocean. Thus, the variability of the Arctic Ocean steric level is an indicator of the ocean upper layer freshening [4]. The method for calculating the steric level from altimetry and GRACE data and its validation is described in [9]. Altimetry data for 2011–2020 in the polar region north of  $81.5^\circ\text{N}$  made it possible to obtain estimates of the steric level for the “blind” spot area (Fig. 2). Figure 5 shows the reconstructed steric level averaged over this area.

The steric level in the “blind” spot area can be considered as an indicator of the freshening/salinization process, since the main contribution to the steric level is made by its halosteric component in the subpolar regions of the ocean. The trend of the steric level in this area is positive and amounts to  $0.3\text{--}0.4$  cm/year (Fig. 5), which indicates an increase in the fresh water supply in 2011–2020.

The reconstructed steric level experiences significant interannual fluctuations and reaches maxima during the negative AO phase, for example, in 2012–2013 and 2015–2017, which indicates an increase in the freshening of water masses (Fig. 5). Accordingly, during the periods of the positive AO phase in 2010–2012 and 2014–2015 minima of the steric level were observed, which indicates an increase in salinity during these periods (Fig. 5). The peculiarity of the steric level variability during the negative AO phase in 2018–2020 should be noted. Thus, the amplitude of fluctuations fell by 3–4 times while keeping a positive trend. This conclusion is confirmed by comparing the content of fresh water in the polar region, calculated from the data of hydrological surveys [4, 5]. Thus, the trend of fresh water content in the upper 100-meter layer for 1994–2008 was  $11.19$  cm/year [4].

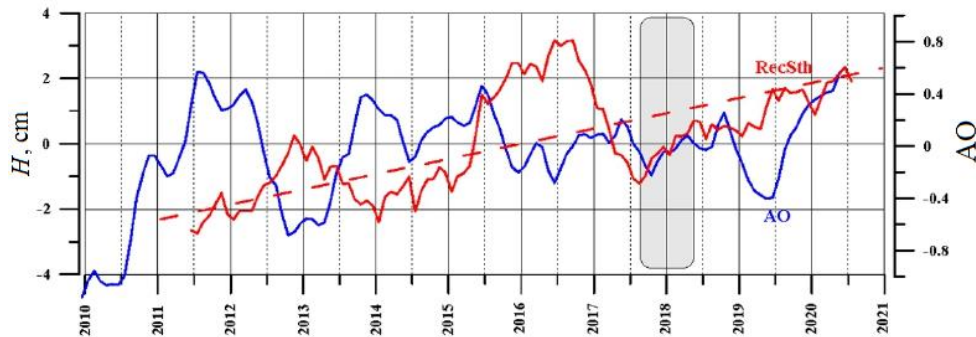


Fig. 5. Plots of the reconstructed steric level (cm) averaged over the area of the “blind” spot (Fig. 1) for 2011–2020 (red solid line), trend (red dashed line), and the AO Index (blue line) after being filtered by a moving average with a window width of 12 months. GRACE data for 07.2017–05.2018 were interpolated (grey area)

The conversion to the steric level was carried out using the constant 35.5 [5], which gives the steric level trend value of 0.34 cm/year and corresponds to the reconstructed steric level trend of 0.3–0.4 cm/year obtained by us.

Similarly, for the area of the Beaufort Gyre (Fig. 1), a positive trend of the reconstructed steric level was obtained (Fig. 6). The value of the trend of the steric level reconstructed from the altimetry and GRACE data was 0.45 cm/year, and the recalculation of the trend of fresh water content in the upper 100-meter layer of the Beaufort Gyre from hydrological data for 1994–2008 gives 0.57 cm/year, which agrees with our estimate with consideration to the error in determining the freshwater content trend [4]. It is interesting to note that the accumulation of fresh water during the positive AO phase was observed in the Beaufort Gyre in 2010–2013, while in 2013–2015, on the contrary, a decrease in the steric level was observed due to the removal of desalinated water from the Beaufort Gyre. After 2015, the accumulation of fresh water had occurred during the negative AO phase, which led to an increase in the steric level (Fig. 6).

The analysis of the atmospheric circulation variability identified by the phases of the AO Index, spatial and temporal variability of the dynamic topography, and reconstructed steric level makes it possible to propose a conceptual scheme of the Arctic Ocean circulation, which is given in Fig. 7. During the negative AO phase, high surface pressure over the Arctic causes anticyclonic circulation over most of the Arctic Ocean (Fig. 7, a). Desalinated waters from the runoff of the Eurasian rivers spread through the Eurasian basin and are carried out of the Arctic Ocean in the region of the Transpolar Drift (Fig. 1), which is shown in Fig. 7, a

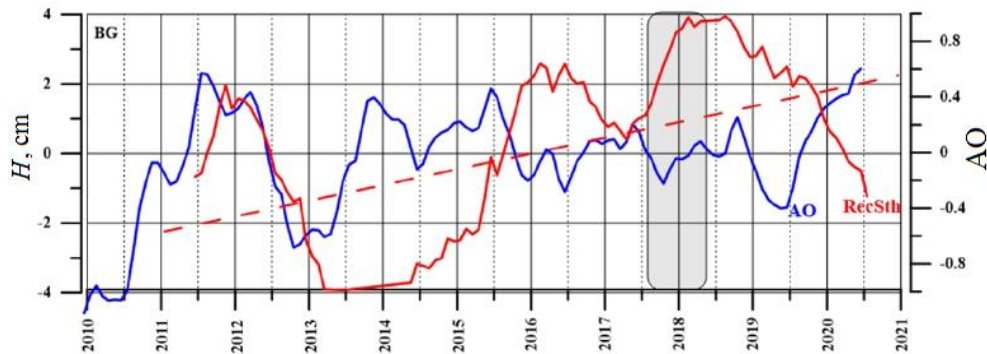


Fig. 6. Plots of the Beaufort gyre area-averaged (Fig. 1) reconstructed steric level (cm) for 2011–2020 (red solid line), its trend (red dashed line) and AO Index after filtering by a moving average with a window width of 12 months. GRACE data for 07.2017–05.2018 were interpolated (grey area)

with dark blue arrows. The analysis of the variability of the reconstructed steric level averaged over the area of the “blind” spot (Fig. 1) shows that it reaches its maximum during the negative AO phase, for example, in 2012–2013 and 2015–2017, which indicates an increase in the freshening of water masses (Fig. 5) and is compliant with the scheme in Fig. 7, *a*. On the other hand, for the area of the Beaufort Gyre, the accumulation of fresh water was also observed during the negative AO phase after 2015 (Fig. 6), which is stipulated by the convergence of the Ekman transport of fresh water on the shelf and is shown by green arrows in Fig. 7, *a* for the Beaufort Gyre, which corresponds to positive values of dynamic topography according to the altimetry data (Fig. 1).

During the positive AO phase, low surface pressure over the Arctic causes cyclonic circulation in the Eurasian basin of the Arctic Ocean (Fig. 7, *b*). Desalinated waters from the flow of the Eurasian rivers spread along the Arctic shelf of Russia by geostrophic currents and the secondary circulation of the ocean and are captured by the Beaufort Gyre, which is shown in Fig. 7, *b* with dark blue and purple arrows. The analysis of the variability of the reconstructed steric level averaged over the area of the “blind” spot shows that during the positive AO phase in 2010–2012 and 2014–2015 minima of the steric level were observed, which indicates an increase in salinity during these periods (Fig. 5) and is compliant with the circulation scheme in Fig. 7, *b*. For the area of the Beaufort Gyre, the accumulation of fresh water was observed during the positive AO phase only in 2011–2013, while in 2013–2015, on the contrary, a decrease in the steric level was observed (Fig. 6). However, for the entire period of 2011–2020, the accumulation of fresh water

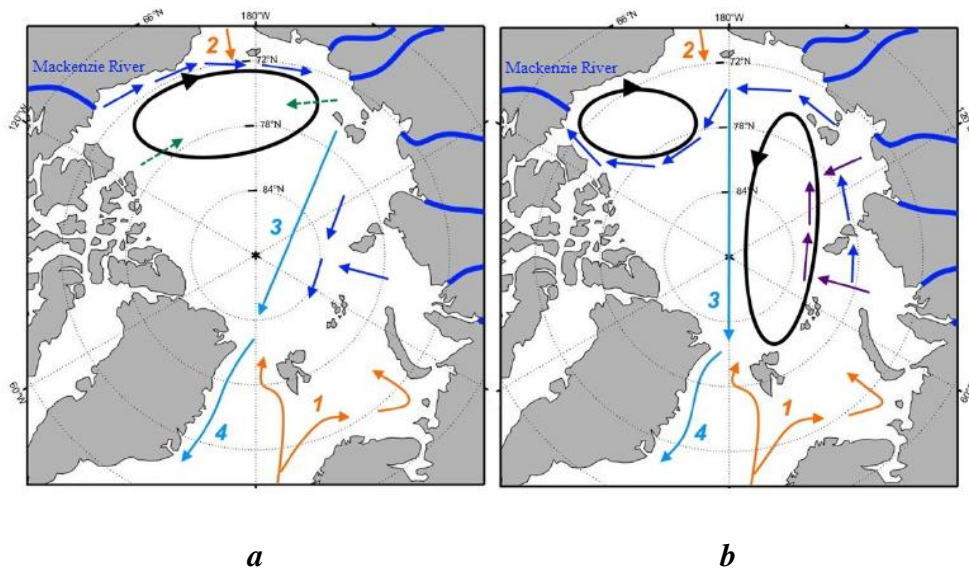


Fig. 7. Conceptual scheme of the Arctic Ocean circulation: (a) during the negative AO phase (anticyclonic,  $AO < 0$ ); b) during the positive AO phase (cyclonic,  $AO > 0$ ). The black arrows indicate surface geostrophic circulation, the orange arrows indicate the inflow of Atlantic (1) and Pacific waters (2); the light blue arrows – Transpolar Drift (3) and East Greenland Current (4). The dark blue and purple arrows show the distribution of fresh water from the Mackenzie River and from the Eurasian Rivers. Green arrows show Ekman transfer of fresh water. The bold dark blue lines are for the rivers flowing into the Arctic Ocean

increased in the Beaufort Gyre as the trend in the steric level was positive (0.45 cm/year), which is also confirmed by the positive trend in freshwater content in the upper 100 m layer of the Beaufort Gyre according to the hydrological data for 1994–2008 [4, 5].

As a result, the proposed conceptual scheme shown in Fig. 7 integrates the results of the analysis of dynamic topography, surface geostrophic currents according to the altimetry data, and reconstructed steric level and AO Index in the context of the influence of atmospheric circulation regimes on the way of fresh water distribution in the Arctic Ocean.

### Conclusion

The change in the level of the Arctic Ocean is an important indicator of climate variability in the Arctic and of the Earth's climate system as a whole due to the integral nature of sea level formation. For the Arctic, progress has been made in the last decade in processing altimetry information and improving its accuracy,

and the launch of the Envisat and CryoSat-2 satellites made it possible to increase the coverage area at high latitudes up to  $89.75^{\circ}\text{N}$ . Therefore, the use of new altimetry data both for the Arctic Ocean regions covered with ice and for the open water area made it possible to obtain the estimates of dynamic topography and surface geostrophic velocities, including the area of the “blind” spot north of  $81.5^{\circ}\text{N}$ , for which altimetry data had not been available until 2011. Using the GRACE gravity data, it was possible to obtain the estimates of the variability of the ocean level manometric and steric components. These estimates are in good agreement with the calculations based on the available instrumental observations. The effect of atmospheric circulation regimes on the spatiotemporal variability of the ocean level and surface currents was studied based on the analysis of the AO Index.

On the basis of the obtained results, a conceptual scheme of the regimes of circulation and distribution of desalinated waters depending on the phase of the Arctic oscillation is proposed. The scheme is compliant with the interannual variability of the reconstructed steric level component for the polar region of the ocean for 2011–2020.

Thus, the main results can be summarized as follows.

1. The spatiotemporal variability of the steric and manometric components of the sea level is specified, and estimates of their trends are obtained from the altimetry, GRACE, and archival hydrological data. Estimates of the steric level variability are obtained for the regions of the Arctic Ocean where the availability of hydrological measurements has been low or almost absent, including the altimetry “blind” spot north of  $81.5^{\circ}\text{N}$  after 2011.

2. The peculiarities of the response of the sea level and surface geostrophic currents of the Arctic Ocean to the cyclonic/anticyclonic circulation of the atmosphere described by the AO Index are characterized.

3. Quantitative estimates of the dependence of the interannual variability of sea level anomalies and surface geostrophic currents are obtained based on regression relationships depending on the value of the AO Index: the level difference between the shelf and the deeper part is  $\sim 4$  cm per AO Index unit, and for current velocity anomalies it is  $\sim 0.6\text{--}0.8$  cm/s per AO Index unit for 2003–2014. This difference increases in the Kara Sea up to  $\sim 5$  cm and to  $\sim 8$  cm per AO Index unit in the  $150\text{--}180^{\circ}\text{E}$  sector (in the Laptev Sea and the East Siberian Sea) in 2011–2020. An increase in level gradients leads to an increase in pressure gradients between the shelf and the deeper part of the ocean and, as a result, to an increase in geostrophic velocities up to  $\sim 1.5$  cm/s per AO Index unit.

Thus, during the positive phase of the AO Index, when the central part of the Arctic is occupied by a cyclone, an increase in the anomalies of current velocities is observed, which contributes to the inflow of warm Atlantic waters. During the negative AO phase, the anomalies of the current velocities reverse.

4. Estimates of trends and interannual variability of the steric component of the level for the area of the “blind” spot north of  $81.5^{\circ}\text{N}$  are obtained for the first time owing to the altimetry and GRACE reconstruction.

5. According to the obtained quantitative patterns, during the negative AO phase, there is an increase in the transport of fresh water from the shelf of the Laptev Sea and the East Siberian Sea to the central part of the ocean. This is confirmed by the interannual variability of the reconstructed steric component of the level averaged over the “blind” spot region north of 81.5°N. As shown, the steric level is an indicator of an increase in freshening/salinization of water masses for the Arctic Ocean. Correspondingly, during the periods of the positive AO phase, minima of the steric level are observed, which indicates an increase in salinity during these periods of time.

6. On the basis of the obtained results, a conceptual scheme of the regimes of circulation and distribution of desalinated waters depending on the phase of the Arctic oscillation is proposed. The scheme is compliant with the ocean circulation regimes based on the analysis of surface geostrophic currents according to the altimetry data and the interannual variability of the reconstructed level steric component for the polar region of the ocean for 2011–2020.

#### REFERENCES

1. Ivanov, V.V., Frolov, I.E. and Filchuk, K.V., 2020. Transformation of Atlantic Water in the North-Eastern Barents Sea in Winter. *Arctic and Antarctic Research*, 66(3), pp. 246–266. doi:10.30758/0555-2648-2020-66-3-246-266
2. Armitage, T.W.K., Bacon, S. and Kwok, R., 2018. Arctic Sea Level and Surface Circulation Response to the Arctic Oscillation. *Geophysical Research Letters*, 45(13), pp. 6576–6584. doi:10.1029/2018GL078386
3. Proshutinsky, A.Y. and Johnson, M.A., 1997. Two Circulation Regimes of the Wind-Driven Arctic Ocean. *Journal of Geophysical Research: Oceans*, 102(C6), pp. 12493–12514. doi:10.1029/97JC00738
4. Pnyushkov, A.V., Alekseev, G.V. and Smirnov, A.V., 2022. On the Interplay between Freshwater Content and Hydrographic Conditions in the Arctic Ocean in the 1990s–2010s. *Journal of Marine Science and Engineering*, 10(3), 401. doi:10.3390/jmse10030401
5. Proshutinsky, A., Krishfield, R., Toole, J.M., Timmermans, M.-L., Williams, W., Zimmermann, S., Yamamoto-Kawai, M., Armitage, T.W.K., Dukhovskoy, D. [et al.], 2019. Analysis of the Beaufort Gyre Freshwater Content in 2003–2018. *Journal of Geophysical Research: Oceans*, 124(12), pp. 9658–9689. doi:10.1029/2019JC015281
6. Raj, R.P., Andersen, O.B., Johannessen, J.A., Gutknecht, B.D., Chatterjee, S., Rose, S.K., Bonaduce, A., Horwath, M., Ranndal, H. [et al.], 2020. Arctic Sea Level Budget Assessment during the GRACE/Argo Time Period. *Remote Sensing*, 12(17), 2837. doi:10.3390/rs12172837
7. Proshutinsky, A., Dukhovskoy, D., Timmermans, M.-L., Krishfield, R. and Bamber, J.L., 2015. Arctic Circulation Regimes. *Philosophical Transactions of the Royal Society A: Mathematical, Physical and Engineering Sciences*, 373(2052), 20140160. doi:10.1098/rsta.2014.0160
8. Belokopytov, V.N., 2017. Factors Reducing Efficiency of the Operational Oceanographic Forecast Systems in the Arctic Basin. *Physical Oceanography*, (2), pp. 19–24. doi:10.22449/1573-160X-2017-2-19-24
9. Lemeshko, E.E., Lemeshko, E.M. and Novitskaya, V.P., 2021. Influence of the Arctic Oscillation on the Formation of Water Circulation Regimes in the Sector of the North, Norwegian and Barents Seas. *Ecological Safety of Coastal and Shelf Zones of Sea*, (2), pp. 47–64. doi:10.22449/2413-5577-2021-2-47-64 (in Russian).



10. Doglioni, F., Ricker, R., Rabe, B., Barth, A., Troupin, C. and Kanzow, T., 2023. Sea Surface Height Anomaly and Geostrophic Current Velocity from Altimetry Measurements over the Arctic Ocean (2011–2020). *Earth System Science Data*, 15(1), pp. 225–263. <https://doi.org/10.5194/essd-15-225-2023>
11. Armitage, T.W.K., Bacon, S., Ridout, A.L., Petty, A.A., Wolbach, S. and Tsamados, M., 2017. Arctic Ocean Surface Geostrophic Circulation 2003–2014. *The Cryosphere*, 11(4), pp. 1767–1780. doi:10.5194/tc-11-1767-2017
12. Volkov, D.L. and Landerer, F.W., 2013. Nonseasonal Fluctuations of the Arctic Ocean Mass Observed by the GRACE Satellites. *Journal of Geophysical Research: Oceans*, 118(12), pp. 6451–6460. doi:10.1002/2013JC009341
13. Peralta-Ferriz, C., Morison, J.H., Wallace, J.M., Bonin, J.A. and Zhang, J., 2014. Arctic Ocean Circulation Patterns Revealed by GRACE. *Journal of Climate*, 27(4), pp. 1445–1468. doi:10.1175/JCLI-D-13-00013.1
14. Morison, J., Kwok, R., Dickinson, S., Andersen, R., Peralta-Ferriz, C., Morison, D., Rigor, I., Dewey, S. and Guthrie, J., 2021. The Cyclonic Mode of Arctic Ocean Circulation. *Journal of Physical Oceanography*, 51(4), pp. 1053–1075. doi:10.1175/JPO-D-20-0190.1
15. Seber, G.A.F., 1980. *Linear Regression Analysis*. New York: Wiley, 465 p.

Submitted 16.12.2022; accepted after review 21.01.2023;  
revised 1.02.2023; published 24.03.2023

*About the author:*

**Egor E. Lemeshko**, Junior Research Associate, Marine Hydrophysical Institute of RAS (2 Kapitanskaya St., Sevastopol, 299011, Russian Federation), **SPIN-код: 7313-4819**; **ResearcherID: C-5691-2016**; **Scopus Author ID: 57205681264**, [e.lemeshko@mhi-ras.ru](mailto:e.lemeshko@mhi-ras.ru)

*The author has read and approved the final manuscript.*